ISBN: 978-3-95450-194-6 ISSN: 2226-0366 doi:10.18429/JACoW-LINAC2018-TH1A01

FIRST EVER IONIZATION COOLING DEMONSTRATION IN MICE

J. Y. Tang*, Institute of High Energy Physics, CAS, 100049 Beijing, China
on behalf of the MICE Collaboration

Abstract

The Muon Ionization Cooling Experiment (MICE) at RAL has studied the ionization cooling of muons. Approximately 350 million of individual particle tracks have been recorded passing through a series of focusing magnets in different configurations with a liquid hydrogen, lithium hydride or polyethylene (wedge) absorber. Measurements of the tracks upstream and downstream of the absorber have shown the expected effects of the 4D emittance reduction as a consequence of ionization cooling. This invited talk presents and discusses these results, and projects the future of ionization cooling.

INTRODUCTION

Muon cooling is one of the basic techniques required for a neutrino factory and muon collider [1]. The international Muon Ionization Cooling Experiment (MICE) at RAL was established to demonstrate the principle and relevant technology [2]. One way of producing high-intensity muons is to collide a high-power proton beam with a target, producing pions that then decay into muons. However, the tertiary muon beam has a very large emittance, typically between 15-20 πmm·rad. In order to optimize the muon yield and fit the beam into cost-effective apertures for further acceleration, one would need to reduce the beam emittance. The desired muon normalized beam emittance at the neutrino factory ranges between 2 and 5 πmm·rad. An initial muon collider needs further cooling with a desired normalized transverse emittance of 0.4 πmm·rad and normalized longitudinal emittance of 1 πmm·rad. Ionization cooling is the only beam cooling technique suitable for reducing the muon beam emittance within the short muon lifetime. MICE successfully demonstrated this technique for the first time.

BEAMLINE

The proton beam used for muon production in MICE is produced by the ISIS proton synchrotron at RAL [3], with a kinetic energy of 800 MeV in a parasitic mode to the operation of the ISIS spallation neutron source and muon source. As shown in Fig. 1, a triplet of quadrupole magnets (Q1, Q2, and Q3), two dipole magnets (D1 and D2), and one decay solenoid (DS) are used for pion transport and proper pion momentum selection, pion decay and muon momentum selection.

Two more triplets prepare the muon beam into the muon cooling channel [4]. As a result, the beam that enters MICE has a small pion content. To ensure further muon beam purity, these pions are tagged and rejected from the cooling measurement using a series of particle identification (PID) detectors (Fig. 2) [5].

* tangjy@ihep.ac.cn

MICE DETECTORS AND ABSORBERS

MICE detectors can be divided into PID and tracking detectors. The primary PID detectors are three Time of Flight (ToF) counters (ToF0, ToF1, and ToF2) made of scintillating slabs. Electrons and pions can be distinguished by their different flight times with the same momentum. In addition, two aerogel Cherenkov detectors help the rejection of pions and electrons. The KLOE-Light (KL) detector is a calorimeter and uses lead layers alternating with scintillating fibers to differentiate between particles based on their energy depositions. Electrons shower in KL and as a result have broader KL distributions compared to muons and pions. The most downstream calorimeter is the Electron Muon Ranger (EMR), made of planes of scintillator extrusions, which makes use of the differing particle track topologies. Electron showers in the EMR typically miss some planes as they travel along their paths (occupancy < 1) in contrast to muon tracks which consistently hit all planes (occupancy ≈ 1) [6].

MICE has two tracking detectors, upstream and downstream of the absorber [7]. Each tracker is composed of five planar scintillating-fiber stations, each with three doublet fiber layers, and is immersed in the solenoidal field of a Spectrometer Solenoid (SS). The upstream and downstream SS consist of five superconducting coils; two match the muon beam into and out of the absorber, and three produce constant fields inside the tracking volumes. For measurement of beam cooling, the input and output beam distributions are compared at the tracker stations immediately upstream and downstream of the absorber (tracker reference planes).

Three kinds of absorbers were used in the cooling experiments, first with lithium hydride (LiH), then liquid hydrogen (LH2) and a wedge type of polyethylene. LiH and LH2 were used to demonstrate the cooling effect in the transverse phase space, and the wedge polyethylene was to demonstrate the emittance exchange between the transverse space and the longitudinal space.

MEASUREMENT OF MUON IONIZATION COOLING

Ionization cooling occurs when muons travel through an absorbing material and undergo a “soft” inelastic collision. With the incoming muon energies significantly larger than the binding energies of the atomic electrons of the material, the atom ionizes, ejecting a valence electron [8]. Concurrent with the ionization energy loss process, elastic collisions with the atomic nuclei of the material can occur. Given the larger mass of the atomic nuclei compared with the incident muons, this process causes very small energy loss [2]. However, it is the driving force behind

ISBN: 978-3-95450-194-6 ISSN: 2226-0366 doi:10.18429/JACoW-LINAC2018-TH1A01

the scattering of muons by small angles [8]. This process is known as multiple Coulomb scattering and is a source of emittance heating that is a counter effect against the cooling.

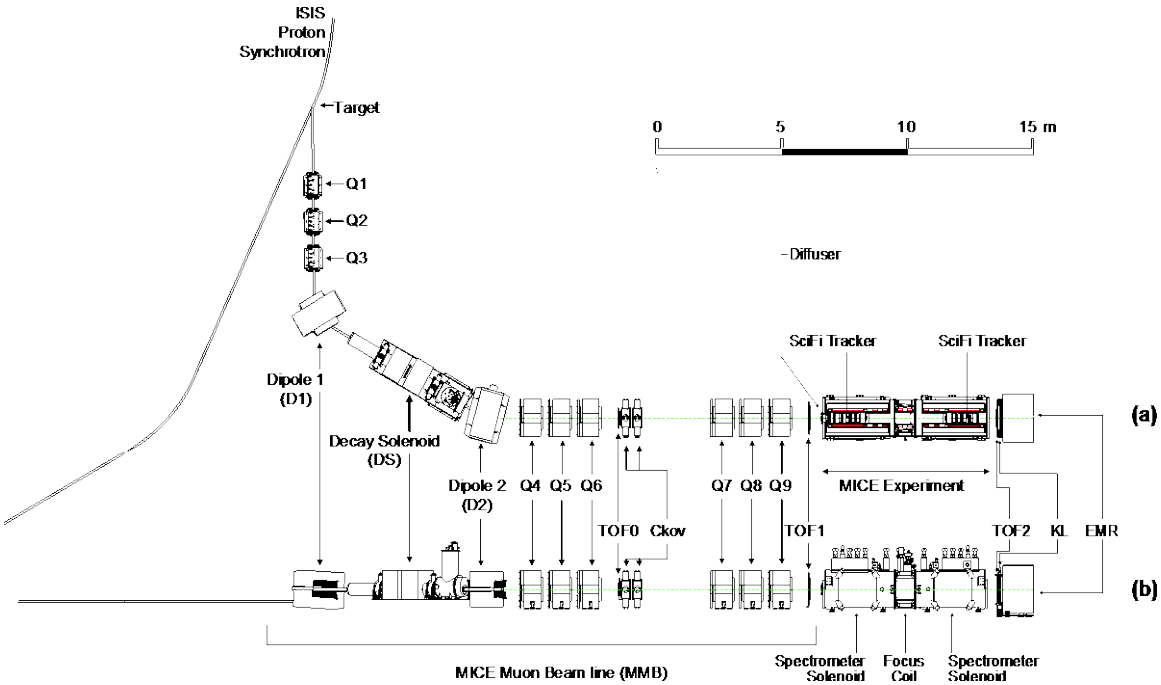

Figure 1: Schematic of the MICE beamline and MICE experiment: (a) and (b) are the top and side views, respectively.

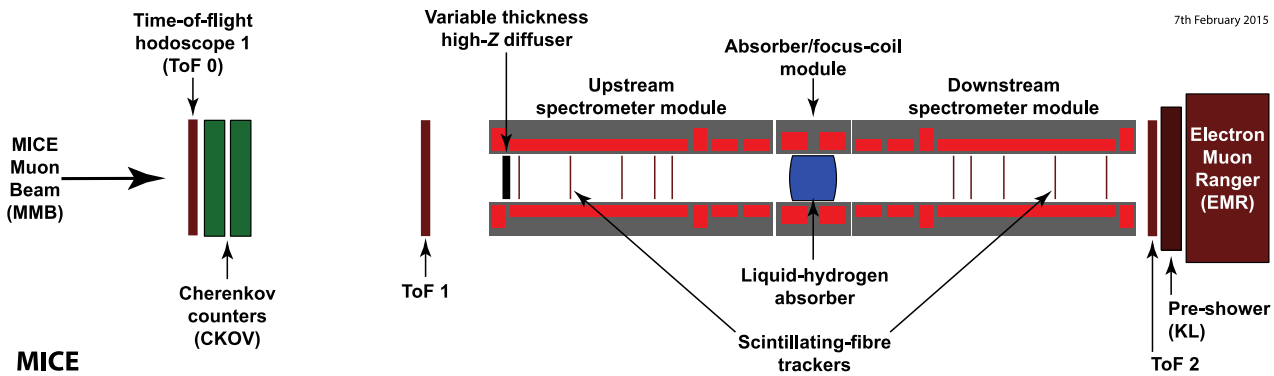

Figure 2: Schematic diagram of MICE in its final configuration.

ISBN: 978-3-95450-194-6 ISSN: 2226-0366 doi:10.18429/JACoW-LINAC2018-TH1A01

A good understanding of energy loss and multiple scattering is essential in ionization cooling where the muon momentum is reduced in all directions (both transversely and longitudinally) with a subsequent restoration of the beam longitudinal momentum in RF cavities, suitable for a multi-segment cooling system. The beam cooling equation that describes this process is written in terms of the rate of change of normalized transverse root-mean-square (RMS) emittance [2]:

$$\frac{d\varepsilon_T}{dz} \cong -\frac{\varepsilon_T}{E_\mu \beta^2}\frac{dE_\mu}{dz} + \frac{\beta_\perp}{2mc^2\beta^3}\frac{(13.6\ \mathrm{MeV/c})^2}{E_\mu X_0}, \quad (1)$$

where E_μ is the muon energy, β the muon velocity, dE_μ/dz the magnitude of the ionization energy loss, m the muon mass, X_0 the radiation length, and $\beta_\perp$ the transverse beta function at the absorber.

The first term in the equation represents cooling from ionization energy loss and the second term describes heating from multiple scattering. The minimum achievable emittance, or equilibrium emittance, for a given material and focusing conditions can be described by:

$$\varepsilon_{eq} \cong \frac{\beta_\perp (13.6\ \mathrm{MeV/c})^2}{2X_0(dE/dz)\beta m}, \quad (2)$$

A smaller equilibrium emittance leads to a more effective emittance reduction, which from Eq. (2) occurs when $\beta_\perp$ is minimized and $X_0(dE/dz)$ maximized [2]. Therefore, strong focusing at the absorber and low-Z (low atomic number) absorbing materials such as lithium hydride and liquid hydrogen are needed.

EXPERIMENTAL RESULTS

One figure of merit for muon beam cooling in MICE is the reduction of the normalized transverse RMS emittance. Muon trajectories are recorded by single particles and the phase-space coordinates in (x, p_x, y, p_y) of each muon are reconstructed using the trackers. From the measured phase-space coordinates, the normalized transverse emittance can be calculated. Figure 3 displays the muon beam emittance versus momentum by using the upstream tracker. The emittance is observed to be approximately constant within the momentum range from 180 to 250 MeV/c.

Though multiple Coulomb scattering is a well-understood phenomenon, results from MUSCAT indicate that the effect in low Z materials is not well modelled in simulations such as GEANT4 [9]. MICE therefore measured the multiple Coulomb scattering distribution to validate the scattering model and determine the heating term in Eq. (1), in order to make more realistic predictions of the emittance reduction. Both data with field off and field on in the scintillating fiber tracker are available for a momentum range of 140-240 MeV/c. While the field-on data is still being analyzed, one preliminary analysis result is shown in Fig. 4.

In addition to emittance reduction, the cooling effect can also be expressed by the reduction of the single-particle amplitude that is defined as the weighted distance of each muon from the beam center. It probes the change in density in the core of the beam, where an increase in phase-space density signifies beam cooling. The transverse beam amplitude can be obtained using the measured transverse emittance [10-12], which causes migration of high amplitude muons to low amplitude and indicates beam cooling, i.e. as $R_{Amp} > 1$ in Fig. 5. Two different input emittances of 6 πmm·rad and 10 πmm·rad, and a momentum of 140 MeV/c were used. The ratio in amplitude change R_{Amp} is defined as:

$$R_{Amp} \equiv \sum_{n=1}^{N} A_n^{down} \Big/ \sum_{n=1}^{N} A_n^{up}, \quad (3)$$

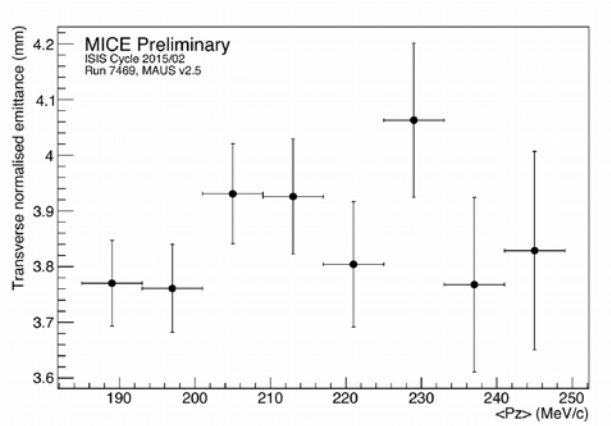

Figure 3: First direct measurement of emittance using the most upstream scintillating fiber tracker station [10].

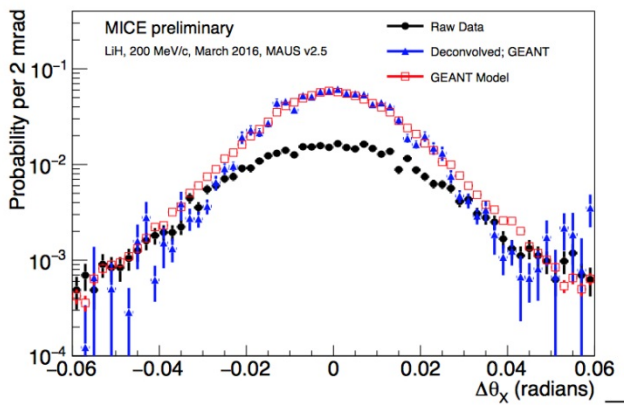

Figure 4: Comparison between experimental multiple Coulomb scattering results and GEANT4 simulations (with LiH, 200 MeV/c).

To express the emittance reduction in 4D-phase space, a fractional emittance that defines the inner phase space volume is used [13-14]. For one RMS emittance in 4D space, which represents about 9% of the total volume, it has a simple relation with the transverse RMS emittance in 2D space:

$$\varepsilon_\alpha = \frac{1}{2}(\pi mc\varepsilon_T)^2 \Rightarrow \frac{\Delta\varepsilon_\alpha}{\varepsilon_\alpha} \approx \frac{2\Delta\varepsilon_T}{\varepsilon_T}. \quad (4)$$

ISBN: 978-3-95450-194-6 ISSN: 2226-0366 doi:10.18429/JACoW-LINAC2018-TH1A01

One experimental result is shown in Fig. 6. One can see the emittance reduction before and after the absorber (LiH).

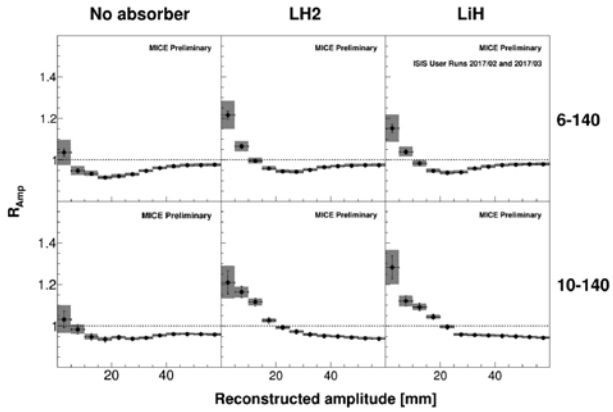

Figure 5: Ratio of cumulative amplitude distributions between upstream and downstream tracker reference plane for the 6-140 (top) and the 10-140 (bottom) nominal beam settings, and three absorber configurations of "no absorber" (empty channel, left), LH2 (middle), and LiH (right).

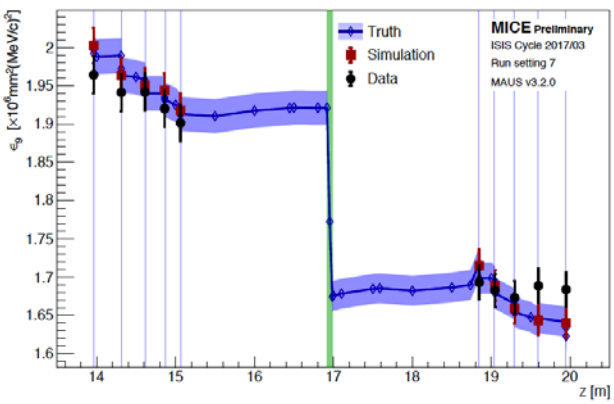

Figure 6: Fractional (9%) emittance evolution (6 πmm·rad, 140 MeV/c, LiH, flip mode)

6D cooling is required by the muon collider, in order to reduce both the transverse and longitudinal emittance for high collision luminosity. One method to produce 6D cooling is to add wedge absorbers in the dispersion location in a cooling section, where the emittance change between the transverse and longitudinal phase spaces happens so the longitudinal emittance cooling is obtained [15]. As there are no magnets producing dispersion in the cooling section, we carried out one experiment by putting a polyethylene wedge in the absorber location (as shown in Fig. 7), and tried to demonstrate reverse emittance change. The reverse emittance exchange is also required by the design of so-called "final cooling" for a multi-TeV muon collider [16]. The data analysis is in progress [17].

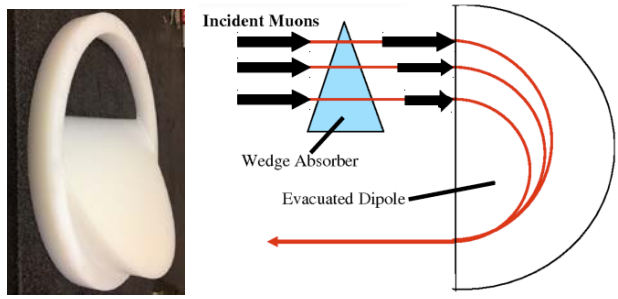

Figure 7: Reverse emittance exchange experiment in MICE: left – polyethylene wedge absorber, right - schematic.

CONCLUSION

The first measurement results of ionization cooling in MICE are presented, and this is an important R&D step towards a future muon collider, neutrino factory, and other cooled muon applications. The measurements of the ratio of the upstream and downstream cumulative amplitude distributions and fractional 4D emittance demonstrate cooling (migration of large transverse amplitude muons to lower amplitudes and emittance reduction after crossing the absorber). MICE has concluded all data taking and is currently in the analysis phase, with several publications in preparation.

ACKNOWLEDGEMENTS

MICE has been made possible by grants from funding agencies from ten participating countries. We acknowledge the support of the staff of the STFC Rutherford Appleton and Daresbury Laboratories, and the use of Grid computing resources deployed and operated by GridPP in the U.K., http://www.gridpp.ac.uk/. The author acknowledges the support from China-US collaboration fund on High-Energy Physics jointly by CAS and IHEP.

REFERENCES

[1] S. Choubey *et al.*, "International Design Study for the Neutrino Factory, Interim Design Report," 2011, arXiv:1112.2853

M. Alsharoa *et al.*, "Recent progress in neutrino factory and muon collider research within the Muon Collaboration," *Phys. Rev. ST Accel. Beams*, vol. 6, p. 081001, 2003.

[2] D. Neuffer, "Principles and applications of muon cooling," *Part. Accel.*, 1983, vol. 14, pp. 75-90, FERMILAB-FN-0378.

[3] C.N. Booth *et al.*, "The design and performance of an improved target for MICE," *JINST*, vol. 11, P05006, 2016.

[4] M. Bonesini *et al.*, "The MICE Muon Beam on ISIS and the beam-line instrumentation of the Muon Ionization Cooling Experiment," *JINST*, vol. 11, P05009, 2012.

[5] P. Soler *et al.*, "Pion Contamination in the MICE Muon Beam," *JINST*, vol. 11, P03001, 2016.

R. Bertoni *et al.*, "The design and commissioning of the MICE upstream time-of-flight system," *Nucl. Instrum. Meth. A*, vol. 615, pp. 14-26, 2010.

ISBN: 978-3-95450-194-6 ISSN: 2226-0366 doi:10.18429/JACoW-LINAC2018-TH1A01

L. Cremaldi *et al*., "A Cherenkov Radiation Detector with High Density Aerogels," *IEEE Trans. Nucl. Sci.*, vol. 56, pp. 1475-1478, 2009.

[6] F. Drielsma *et al*., "Electron-Muon Ranger: performance in the MICE Muon Beam," *Journal of Instrumentation,* vol. 10, P12012, 2015.

[7] M. Ellis *et al.*, "The design, construction and performance of the MICE scintillating fibre trackers," *Nucl. Instr. Meth. Phys. Res. A*, vol. 659, p. 136-153, 2011.

[8] C. Patrignani *et al*., (Particle Data Group), *Chin. Phys. C,* vol. 40, p. 100001, (2016, 2017 update).

[9] D. Attwood *et al.*, "The scattering of muons in low Z materials," *Nucl. Instrum. Meth. B*, vol. 251, p. 41, 2006.

MuScat Collaboration, W. J. Murray, "Comparison of MuScat data with GEANT4", *Nucl. Phys. Proc. Suppl.*, vol. 149, p. 99-103, 2005.

[10] V. J. Blackmore, "Emittance Measurement in the Muon Ion- ization Cooling Experiment", *PoS ICHEP2016*, 868 (2016).

[11] C.T. Rogers, "Study of Ionization Cooling with the MICE Experiment," in *Proc. 8th Int. Particle Accelerator Conf. (IPAC'17)*, Copenhagen, Denmark, May 2017, paper WEPAB129.

[12] V. J. Blackmore, "Recent Results from the Study of Emittance Evolution in MICE," in *Proc. 9th Int. Particle Accelerator Conf. (IPAC'18)*, Vancouver, BC, Canada, Apr.-May 2018, paper TUPML067.

[13] T.A. Mohayai, "First demonstration of ionization cooling in MICE", in *Proc. 9th Int. Particle Accelerator Conf. (IPAC'18)*, Vancouver, BC, Canada, Apr.-May 2018, paper FRXGBE3.

[14] D. Rajaram, V. Blackmore, "Phase space density evolution in MICE", in *Proc. 9th Int. Particle Accelerator Conf. (IPAC'18)*, Vancouver, BC, Canada, Apr.-May 2018, paper TUPML065.

[15] D. Kaplan, "Overview of muon cooling", in *Proc.* COOL2015, Newport News, VA, USA, 2015, paper MOWAUD03.

[16] D. Neuffer, "Phase Space Exchange in Thick Wedge Absorbers for Ionization Cooling", *AIP Conference Proceedings,* vol. 441. pp. 270-281. 1998.

[17] T. A. Mohayai *et al*., "A Wedge Test in MICE", in *Proc. 9th Int. Particle Accelerator Conf. (IPAC'18)*, Vancouver, BC, Canada, Apr.-May 2018, arXiv:1806.01824